

CHAPTER 2

Theory

Principally, an ORC is similar to the steam Rankine cycle but uses a refrigerant instead of water. A steam Rankine cycle can be used when a high-temperature heat source is available while ORC can be used when low or medium temperature heat source is available. The input heat to ORC can be supplied from a low-grade energy source. ORC can be integrated with a turbine, as an example of a system that is based on a non-renewable energy source. Also, ORC can be integrated with solar thermal, biomass, waste heat, or geothermal energy as an example of a system that is based on a renewable energy source. This study helps in evaluating the feasibility of using low-temperature heat source for drive turbine on ORC in basic cycle generation systems.

2.1 Thermodynamics of Organic Rankine Cycle

2.1.1 First and Second Law of Thermodynamics

A basic ORC system for converting low-temperature heat sources into useful electrical power is depicted in Figure 2.1(a), 2.1(b) and 2.1(c). The system consists of four processes; (i) increasing pressure of the working fluid through a pump, (ii) high-temperature heat addition through an vapor generator, (iii) expansion of the high temperature as well as high pressure fluid through a turbine, and (iv) low-temperature heat rejection through a condenser. In case of isentropic fluids, the state point after the expansion in the turbine lies in the superheated vapor region. As the temperature of the saturated vapor at the turbine outlet is more than that of the liquid at the inlet of the vapor generator, it is possible to improve thermal efficiency of the cycle through a regenerator. The temperature of the vapor generator feed can be further increased by bleeding of working fluid from the turbine and mixing it with the vapor generator feed in a direct contact heater. Simultaneous regeneration and turbine bleeding improves the internal heat exchanger is incorporate into the ORC. The schematic of an ORC incorporating both regeneration and turbine bleeding is show in Figure 2.1(d) (Desai, et al 2009).

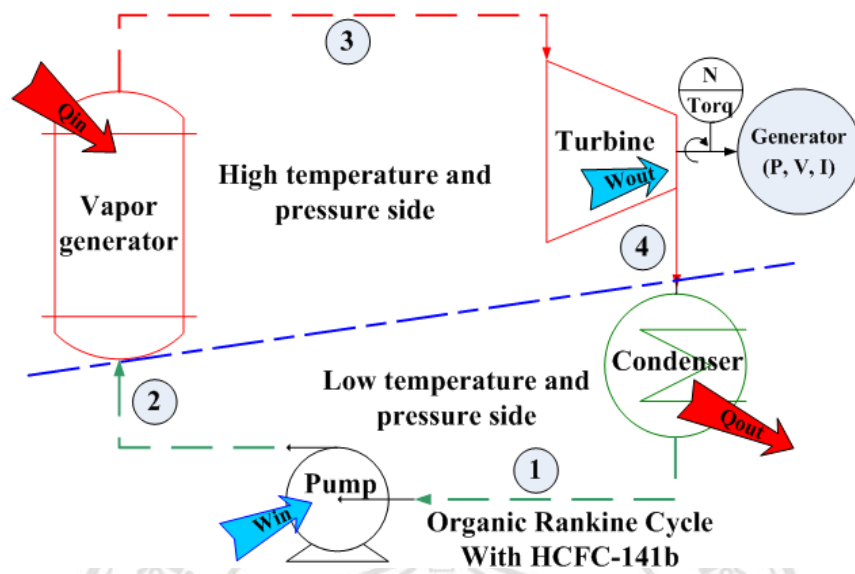


Figure 2.1(a): Basic ORC system for converting waste heat from low heat sources into electrical power

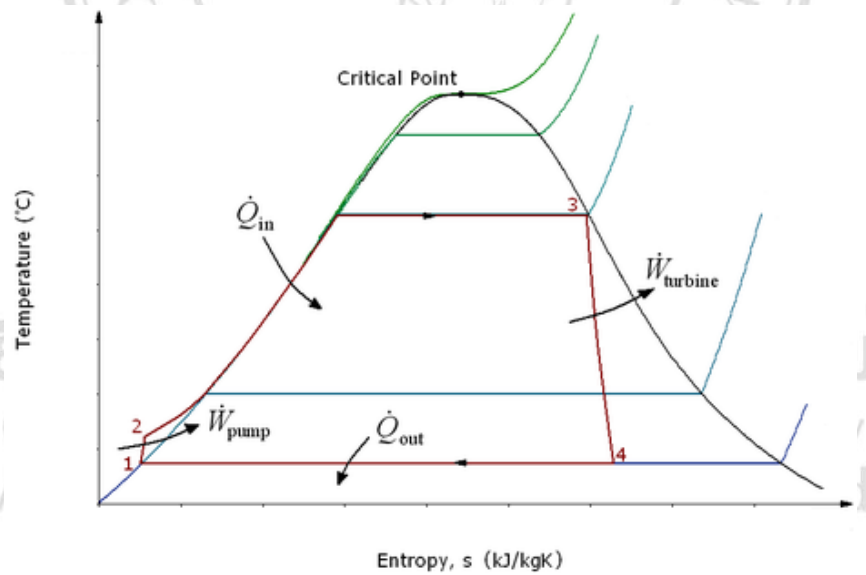


Figure 2.1(b): Schematic of T-s diagram on ORC (Cengel and Bole, 2002)

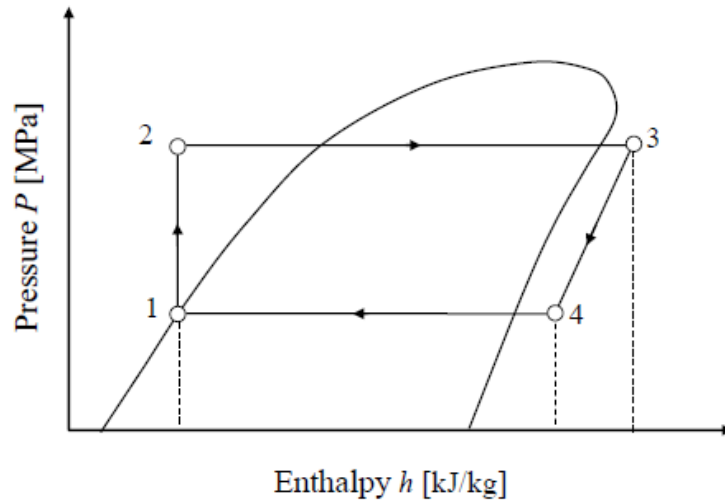


Figure 2.1(c): Schematic of P-h diagram on ORC (Musthafah *et al*, 2010)

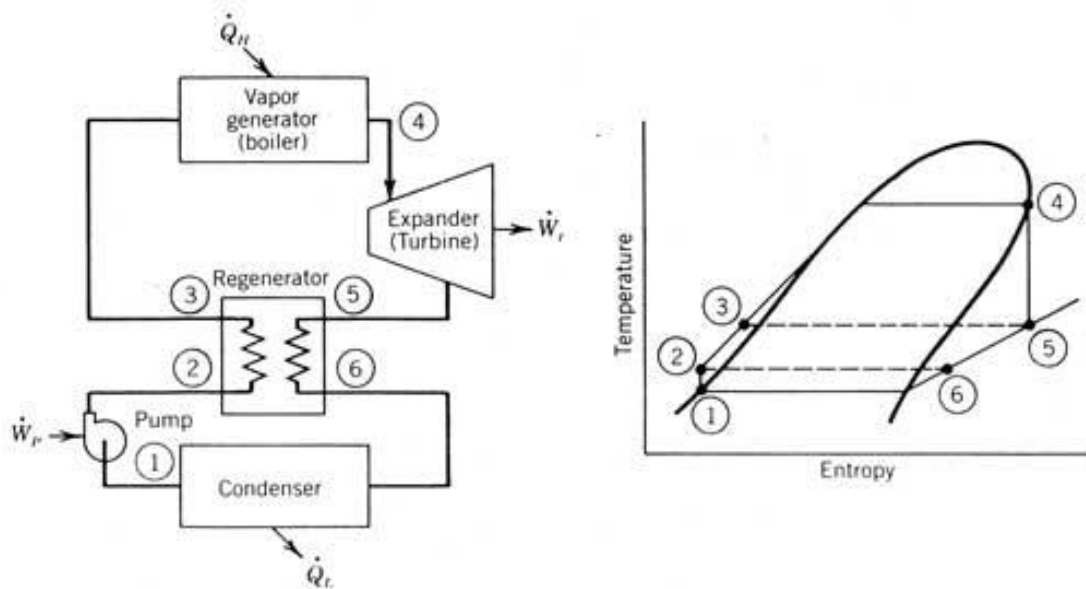


Figure 2.1(d): Schematic of ORC incorporating both regeneration and turbine bleeding (Li *et al*, 2013)

Figure 2.1: Principle of organic Rankine cycle (a) Basic ORC, (b) T-s diagram, (c) P-h diagram, and (d) Regeneration ORC

The theories used to determine the cycle efficiencies as well as the cycle irreversibility for ORC configurations are presented in this section. The thermodynamic model presented in this chapter assumes the following status:

- 1) Steady state conditions,
- 2) No-pressure drop in the vapor generator, condenser, and pipes, and
- 3) Isentropic efficiencies for the turbine and pump.

The components of a basic ORC for converting low-temperature heat into useful power generate are shown in Figure 2.1(a) as observed in the basic ORC consists of four different processes:

- Process 1 – 2 is the pumping process in the pump.
- Process 2 – 3 is the constant pressure heat addition in the vapor generator.
- Process 3 – 4 is the expansion process in the turbine.
- Process 4 – 1 is the constant pressure heat rejection in the condenser.

For each component, the first and second laws of thermodynamic are applied to find the work output, the heat added or rejected, and the components and system irreversibility. The conservation of energy equation applied to every device is,

$$\sum_i E_i + \dot{Q} = \sum_o E_o + \dot{W} \quad 2.1$$

Where E_i and E_o are the energy rate inlet and outlet, kW

\dot{Q} is the heat transfer rate, kW

\dot{W} is the work rate, kW

The irreversibility rate for uniform flow conditions is given by

$$\dot{I} = T_o \frac{dS}{dt} = T_o \dot{m} \left[\sum s_{out} - \sum s_{in} + \left(\frac{ds_{sys}}{dt} \right) + \sum_k \frac{q_k}{T_k} \right] \quad 2.2$$

where k is the heat transfer for different reservoirs and $\frac{ds_{sys}}{dt} = 0$ for steady state conditions.

2.1.2 Simulation Model of the Organic Rankine Cycle

The simulation models of ORC are developed for system designing and analysis. The first simulation model is designed for rapid screening of potential power cycle configurations and the second for detailed simulation, optimization and analysis.

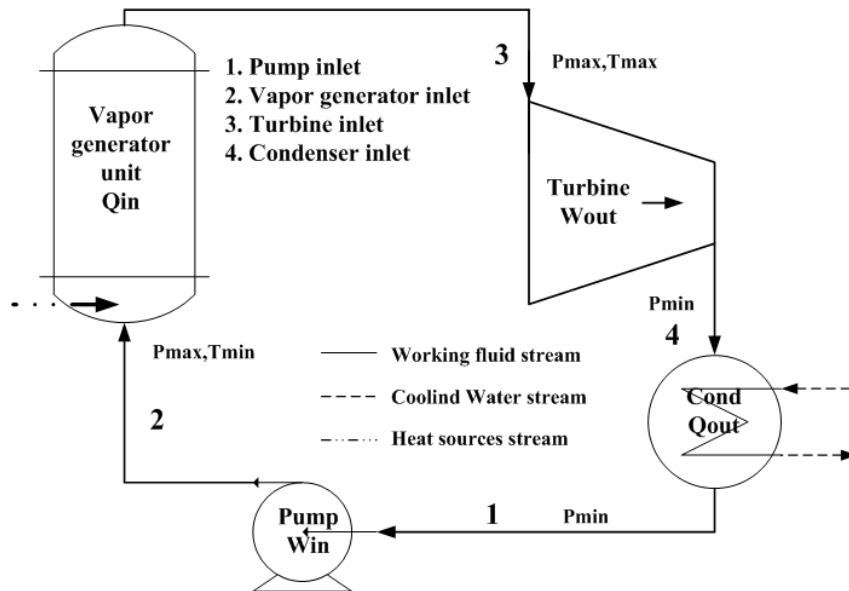


Figure 2.2: Simulation model components of ORC with single-stage turbine

The cycle analysis model is designed to compare and evaluate potential ORC configuration. The equations that describe the performance of each cycle component are developed and the coupled equations are solved to provide a steady state operating point that can be analyzed to determine the performance potential of a particular cycle. The model described first in this section is the most common ORC configuration, a single-stage expansion. This cycle configuration will be referred to as the basic cycle.

This simulation model requires the following parameters to identify a steady-state operating point:

- The vapor generator approach temperature (pinch-point).
- The water cooled condenser approach temperature (pinch-point).
- The working fluid mass flow rate.
- The components pressure drop.

- The heat source and cooling water temperature.
- Heat transfer fluid supply temperature.
- Pump and turbine efficiencies.
- Assume steady state, no heat loss and pressure drop in the entire system.

Process 1-2 (Pump): The liquid leaving the condenser at Point 1 is pumped into the Vapor generator. The pump performance is governed by an isentropic efficiency. Figure 2.3 show the fluid flows associated with the pump.

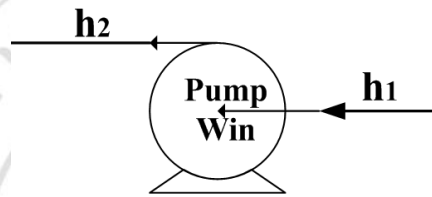


Figure 2.3: Fluid flow pump diagram

Taking a control volume around the pump, using Equation 2.3 and assuming a pump isentropic efficiency, the power of pump can be expressed as follow,

$$\dot{W}_p = \frac{\dot{W}_{p,ideal}}{\eta_p} = \frac{\dot{m}(h_1 - h_{2s})}{\eta_p} \quad 2.3$$

where $\dot{W}_{p,ideal}$ is the ideal power of the pump, \dot{m} is the working fluid mass flow rate, η_p is the pump isentropic efficiency, and h_1 and h_{2s} are the enthalpies of working fluid at the inlet and outlet of the pump for the ideal case.

The exergy balance for the pump is give by:

$$\dot{W}_p = T_0 \dot{S}_{gen} = T_0 \dot{m}(s_2 - s_1) \quad 2.4$$

The pump irreversibility rate can be determined as,

$$\dot{I}_{destroyedp} = T_0 \dot{S}_{gen} = T_0 \dot{m}(s_2 - s_1) \quad 2.5$$

where s_1 and s_2 are the specific entropies of the working fluid at the inlet and outlet of the pump for the actual conditions, respectively.

The second law efficiency is:

$$\eta_{II,p} = 1 - \frac{\dot{I}_{d,p}}{\dot{m}(h_1 - h_{2s})} = \frac{W_p}{\dot{m}(h_1 - h_{2s})} \quad 2.6$$

where h_1 and h_{2s} are the specific enthalpies of the working fluid at the inlet and outlet of the pump for the actual conditions, respectively.

Process 2-3 (Vapor generator): The vapor generator is modeled such that all power cycle heat addition takes place in a single adiabatic heat exchanger. Figure 2.4 shows the flows through the vapor generator, where h refers to fluid enthalpy and the subscript refers to the state point shown in Figure 2.4.

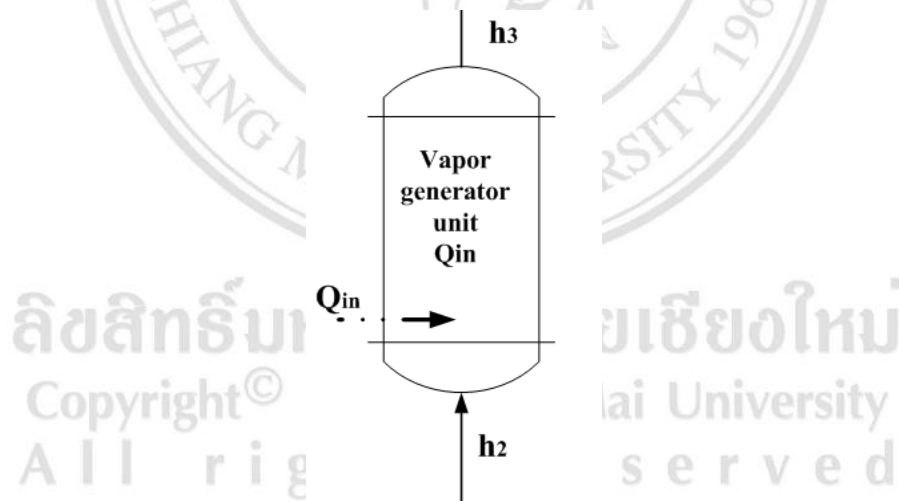


Figure 2.4: Flow direction of working fluid through vapor generator

The performance of the vapor generator is constrained by the heat exchanger pinch-point parameter, where the pinch-point temperature is defined as the minimum temperature difference occurring in the heat exchanger. In most cycles this occurs at the working fluid liquid saturation point, as shown in Figure 2.5, or at the working fluid outlet.

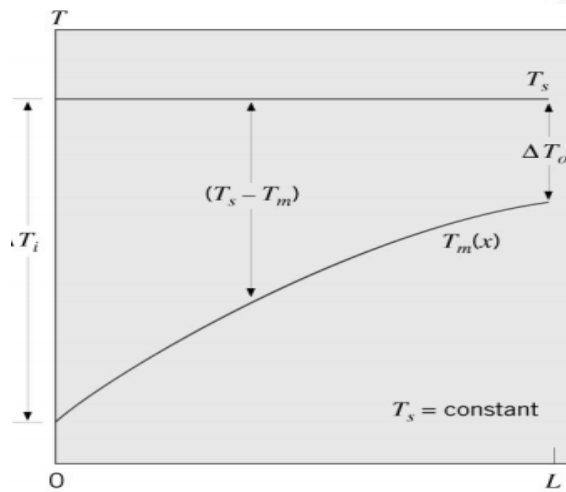


Figure 2.5: Vapor generator pinch-point temperatures (Incropera, 2005)

The energy balance on vapor generator heats the working fluid from the pump outlet to the turbine inlet condition. A control volume enclosing the vapor generator, the heat transfer rate from the energy source into the working fluid is given,

$$\dot{Q}_{vg} = \dot{m}(h_3 - h_2) \quad 2.7$$

where h_2 and h_3 are the enthalpies of the working fluid at the inlet and outlet of the vapor generator, respectively.

In order to predict of the vapor generator performance in the simulation model a log mean temperature difference approach is such that,

$$\dot{Q}_{vg} = U_{vg} A_{vg} \Delta T_{LM,vg} \quad 2.8$$

where $U_{vg} A_{vg}$ is the heat transfer coefficient heat exchanger area product and $\Delta T_{LM,vg}$ is the log-mean temperature difference defined as (Incropera, 2002),

$$\Delta T_{LM,vg} = \frac{(T_{h,i} - T_{c,o}) - (T_{h,o} - T_{c,i})}{\ln \left(\frac{T_{h,i} - T_{c,o}}{T_{h,o} - T_{c,i}} \right)} \quad 2.9$$

The vapor generator irreversibility rate can be determined as,

$$\dot{i}_{vg} = T_o \dot{m} \left[(s_3 - s_2) - \frac{h_3 - h_2}{T_h} \right] \quad 2.10$$

where s_3 and s_2 are the specific entropies of the working fluid at the inlet and exit of the vapor generator, respectively, and T_h is the temperature of the high-temperature heat source. This temperature is considered to be equal to $T_h = T_3 + \Delta T_h$

Process 3-4 (Turbine): Vapor from the vapor generator at point 3, with a high temperature and pressure, expands through the turbine to produce mechanical work and then is passed to the condenser at point 4.

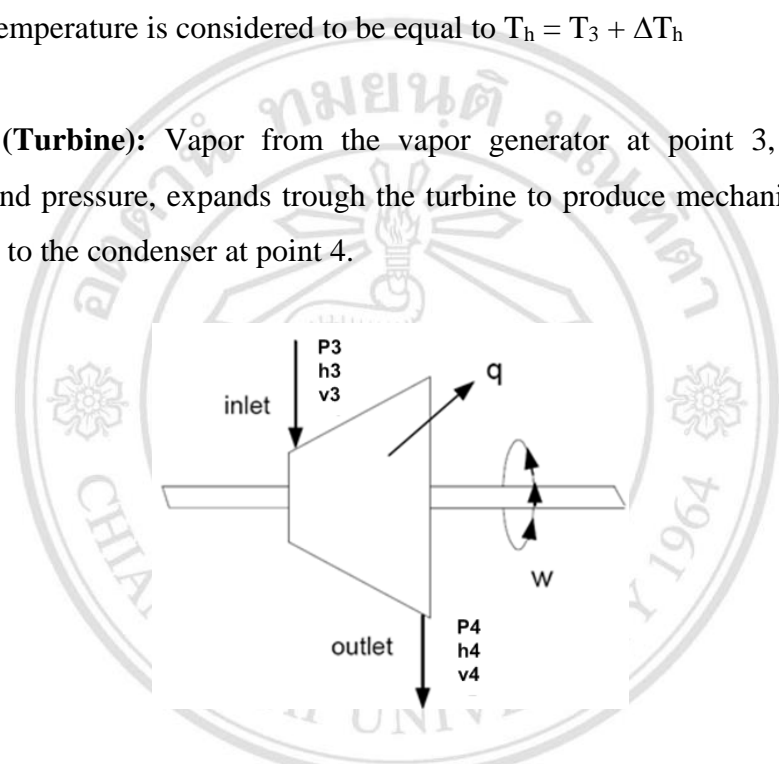


Figure 2.6 (a): Process flow diagram

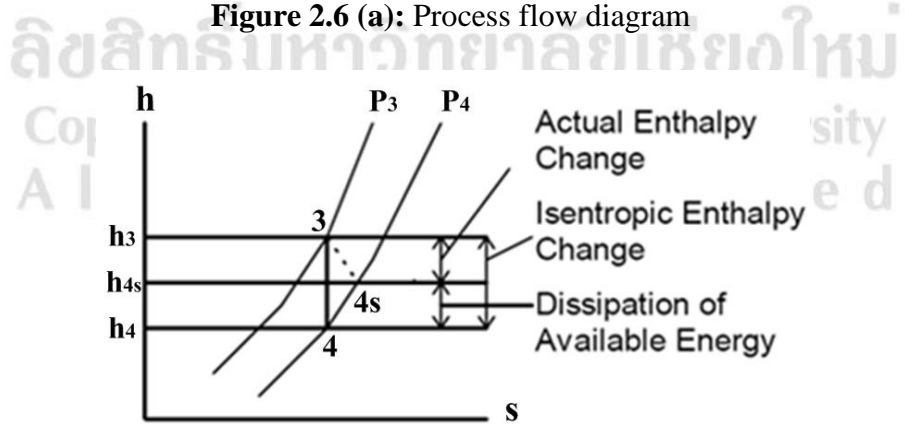


Figure 2.6 (b): h-s diagram on the turbine

Figure 2.6: Turbine flow process (Kapooria. *et al.*, 2008)

The turbine is modeled using an isentropic efficiency for the turbine and a mechanical into electrical efficiency to describe its performance. Figure 2.6 shows the turbine generator and related working fluid enthalpies.

The turbine power output for this configuration is given by,

$$\dot{W}_t = \dot{W}_{t,\text{ideal}} \eta_t = \dot{m}(h_3 - h_{4s}) \cdot \eta_t \quad 2.11$$

The turbine isentropic efficiency is defined as follows (Moran *et al.*, 2002),

$$\eta_t = \frac{h_3 - h_4}{h_3 - h_{4s}} \quad 2.12$$

where $\dot{W}_{t,\text{ideal}}$ is the ideal power of the turbine, η_t is the turbine isentropic efficiency, and h_3 and h_{4s} are the enthalpies of the working fluid at the inlet and outlet of the turbine for the ideal case. The turbine irreversibility rate is,

$$\dot{I}_t = T_o \dot{m}(s_4 - s_3) \quad 2.13$$

where s_3 and s_4 are the specific entropies of the working fluid at the inlet and exit of the turbine for the actual conditions, respectively.

Process 4-1 (Condenser): the condenser is governed by a pinch-point temperature parameter. The pressure at point 4 is the saturation pressure corresponding to the condensing temperature. Figure 2.4 shows the flows associated with the condenser.

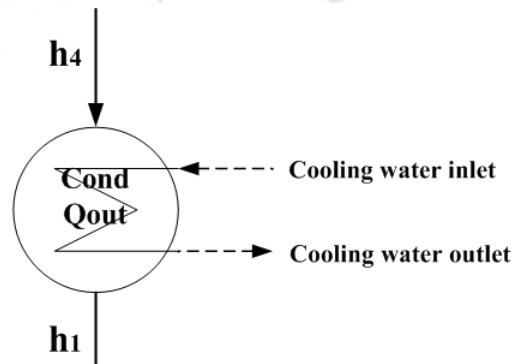


Figure 2.7: Flow directions in condenser

Total condenser heat rejection rate and cooling outlet conditions are again calculated with an energy balance can be expressed as,

$$\dot{Q}_c = \dot{m}(h_1 - h_4) \quad 2.14$$

The condenser irreversibility rate can be determined as follows,

$$\dot{I}_c = T_o \dot{m} \left[(s_1 - s_4) - \frac{h_1 - h_4}{T_1} \right] \quad 2.15$$

where s_1 and s_4 are the specific entropies of the working fluid at the inlet and exit of the condenser, respectively, and T_1 is the temperature of the low temperature reservoir. This temperature is considered to be equal to $T_1 = T_1 - \Delta T_1$.

Cycle efficiency: The thermal efficiency is defined as the ratio between the net powers of the cycle to the vapor generator heat rate. It gives a measure about how much of the waste heat input to the working fluid passing through the vapor generator is converted to the net work output and can be expressed as,

$$\eta_{\text{cycle}} = \frac{\dot{W}_t + \dot{W}_p}{\dot{Q}_{\text{vg}}} \quad 2.16$$

Substituting Equations (2.3), (2.5), and (2.7) into Equation (2.11) the thermal efficiency for a basic ORC can be written as,

$$\eta_{\text{cycle}} = \frac{(h_3 - h_{4s}) \cdot \eta_t + (h_1 - h_{2s}) \cdot \eta_p^{-1}}{(h_3 - h_2)} \quad 2.17$$

Total-Cycle Irreversibly:

The total irreversibility can be obtained adding Equations (2.4), (2.6), (2.8), and (2.10) as follows,

$$\dot{I}_{\text{cycle}} = \sum_j \dot{I}_j = \dot{I}_p + \dot{I}_{\text{vg}} + \dot{I}_t + \dot{I}_c = T_o \dot{m} \left[-\frac{h_3 - h_2}{T_H} - \frac{h_1 - h_4}{T_L} \right] \quad 2.18$$

Second-Law Efficiency:

The second law cycle efficiency can be calculated using the following equation,

$$\eta_{II} = \frac{\dot{W}_{net}}{\dot{Q}_{vg} \left(1 - \frac{T_c}{T_h}\right)} = \frac{(h_3 - h_{4s}) \cdot \eta_t + (h_1 - h_{2s}) \cdot \eta_p^{-1} \left(1 - \frac{T_c}{T_h}\right)^{-1}}{(h_3 - h_2)} \quad 2.19$$

Electric Generator: The mechanical power produced in the turbine is converted to electric power in the generator. The total electric power is,

$$\dot{W}_e = \dot{W}_{net} \cdot \eta_{gen} = (\dot{W}_t + \dot{W}_p) \cdot \eta_{gen} \quad 2.20$$

where η_{gen} is the generator efficiency.

2.2 Working Fluids for the ORC

A Rankine cycle system, using an organic fluid instead of water as the working fluid, It is potentially feasible in heat recovery systems and is particularly favorable in low-temperature applications. Many actual applications have been installed for recovering low-temperature heat for power generation (Lui *et al.*, 2004). However, the selection of working fluids and operation conditions are very important to system performance. The thermodynamic properties of working fluids will affect the system efficiency, operation, and environmental impact.

2.2.1 Working Fluid Selection for Low-Temperature Heat Sources

The working fluid is an important part of Rankine cycle plant. Thermodynamics properties of the working fluids are key parameters for modeling of the system (Kohler *et al.*, 2003). In order to get the maximum out of a refrigerant, the refrigerant should satisfy some very important requirements. For ORC applications, flammable compounds could be employed if appropriate safety measures are permitted. Working fluids which are phased out are neglected owing to their high ozone depletion potential (Angelino *et al.*, 1998). Also there are some general criteria (Vijayaraghavan

et al., 2005) like stability of the fluid, non-fouling nature, non-corrosiveness etc. To improve the heat transfer characteristics, the thermal conductivity of the selected refrigerants has to be high. The latent heat of vaporization should be high which means a smaller flow rate is required for a similar output from the plant. The liquid specific heat should be high meaning that less preheating is required (Vijayaraghavan *et al.*, 2005). In addition to the above mentioned characteristics, there are many more features which will improve the heat transfer capability and thermo-physical performance of the plant that are worth mentioning. They are high molecular weight, low specific volume, moderate vapor pressure in the heat exchanger units, low viscosity and surface tension, suitable thermal stability limits, compatibility with engine materials, and low cost.

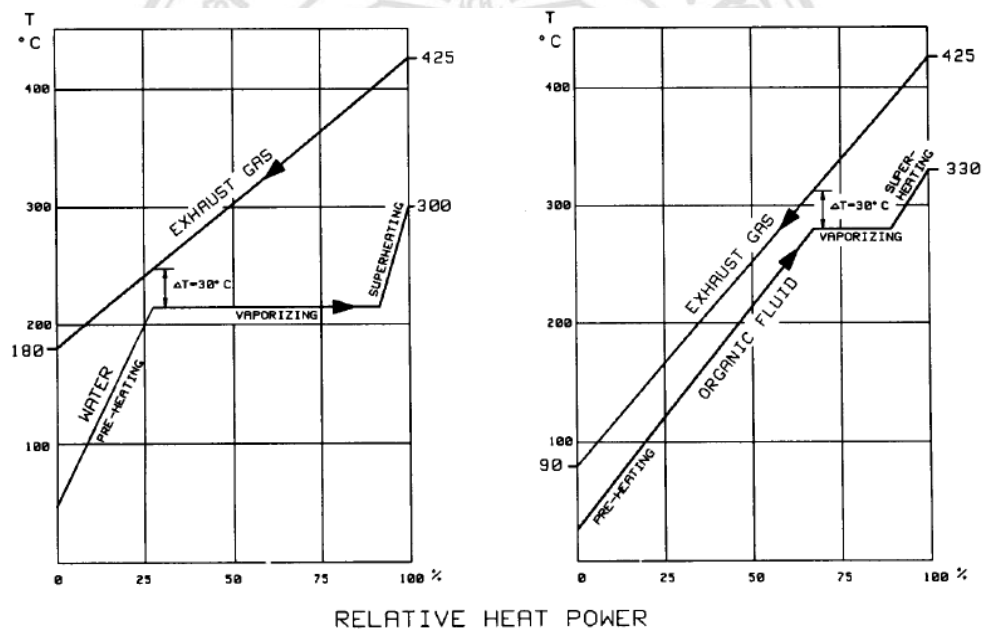


Figure 2.8: Specific heat of vaporization of working fluid (Lajola, 1995)

Typical saturation vapor curves for different fluids depending on the slope of the T-s curve (dT/ds) to be positive, infinite, and negative are shown in Figure 2.9. Fluids, based on the saturation vapor curve on the T-s diagram, may be classified into three groups; (a) dry fluids such as n-pentane, benzene, toluene, etc., having a positive slope as show in Figure 2.9(a), (b) wet fluids such as water, ammonia, etc., having a negative slope as show in Figure 2.9(b), and (c) isentropic fluids such as trichlorofluoromethane, dichlorodifluoromethane, etc., having an infinite slope as shown in Figure 2.9(c).

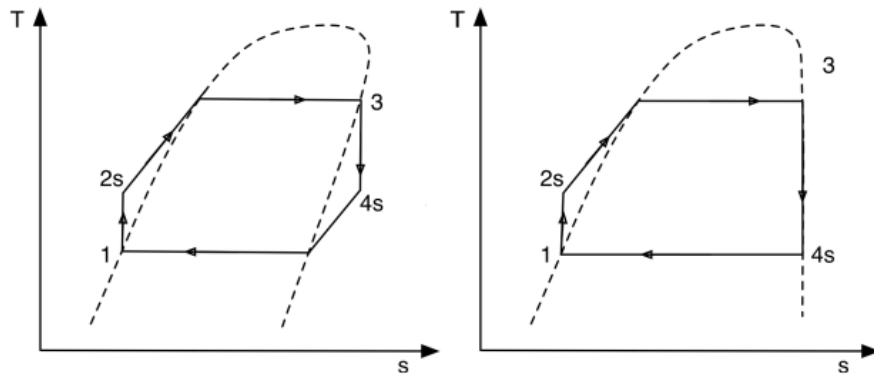


Figure 2.9 (a): Dry fluid

Figure 2.9 (b): Isentropic fluid

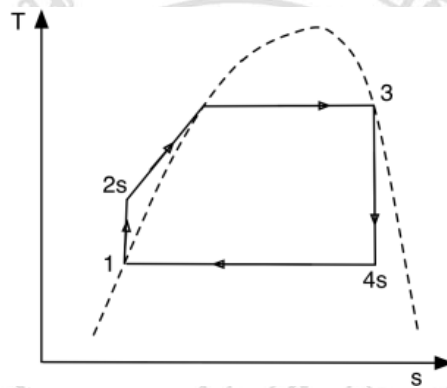


Figure 2.9 (c): Wet fluid

Figure 2.9: Typical saturation curves on T-s diagram (Somayaji *et al.*, 2008).

In a basic Rankine cycle, a fluid expands isentropically through the turbine to produce powers. Due to the negative slope of the saturation vapor curve for a wet fluid, outlet stream of the turbine typically contains lot of saturated liquid. Presence of liquid inside turbine may damage turbine blades and it also reduces the isentropic efficiency of the turbine. Due to reduction in heat transfer coefficient in the vapor phase, heat transfer area requirement and hence, the cost of the superheated goes up significantly. There are other operational issues related to the superheated as well. On the other hand, dry and isentropic fluids do not offer such disadvantages as the condition of the expanded stream at the turbine outlet is always either saturated or superheated vapor. Therefore, the dry and the isentropic fluids are most preferred working fluid for the ORC system which utilizes low grade heat sources (Wei *et al.*, 2007). Hung *et al.* (2001) have shown that the thermal efficiency of the ORC slightly decreases with superheating in case of

dry fluids. Therefore, the dry working fluids are operated at the saturated conditions without being superheated. Mago *et al.* (2007) concluded that the specific irreversibility increases and the second-law efficiency decreases with superheating a dry working fluid operated ORC.

The working fluids of dry or isentropic type are more appropriate for ORC systems. This is because dry or isentropic fluids are superheated after isentropic expansion, thereby eliminating the concerns of impingement of liquid droplets on the turbine blades. Moreover, the superheated apparatus is not needed. Many analyses of the influence of working fluids on the system efficiency were reported in the literature (Hung *et al.*, 1997). Attempts were made to examine various types of working fluids, such as dry, isentropic, and wet ones, and effect of working fluids on system efficiency by equation of state and correlation based on experimental data. Nevertheless, these analyses are difficult to apply since their results may lack of intuitive explanation and simple expressions. When a constant temperature prevails along an evaporator, Hung *et al.*, (2001) showed that the irreversibility of the system depends on the types of working fluids and of heat sources. A system with lower irreversibility results in a better performance. In practice, the temperature of the waste heat medium varies along an evaporator, rather than remaining constant. By incorporating the effect into the analysis, Larjola, (1995) pointed out that higher power output is obtainable when the working fluid “follows” better the heat source fluid to be cooled. In other words, a system has a better performance if the temperature difference between the heat source and the temperature of the working fluid in an evaporator is reduced due to its lower irreversibility.

2.2.2 Analysis of Working Fluids for Low-Temperature Power Cycle

The thermodynamic relation of entropy is described by

$$ds = \frac{C_p}{T} dT - \left(\frac{\partial V}{\partial T} \right)_p dP \quad 2.21$$

As shown in Figure 2.10, the reference state ($S = 0$) is at $T = T_{ref}$ and $P = P_{ref}$ which is in fact a sub-cooled liquid state. The entropy of the saturated vapor (state 3) can be expressed as,

$$s = - \int_{T_R, P_R}^{T_h, P_h} \left(\frac{\partial V}{\partial T} \right)_P dP + \int_{T_R, P_R}^{T_h, P_h} \left(\frac{C_P}{T} \right) dT + \frac{\Delta h_h}{T_h} \quad 2.22$$

where ΔH_H , T_H , and P_H denote the enthalpy of vaporization, the vaporizing temperature, and the vaporizing pressure, respectively. The RHS in Equation 2.20 denotes the integral from the reference state (T_{ref} , P_{ref}) to state ref (T_{ref} , P_h), state ref (T_{ref} , P_h) to state 22 (T_h , P_h), then state 22 (T_h , P_h) to state 3 (T_H , P_H). During the integration, the heat capacity of liquid C_P is relatively independent of pressure and of the incompressibility of the liquid $(\partial V / \partial T)_P = 0$.

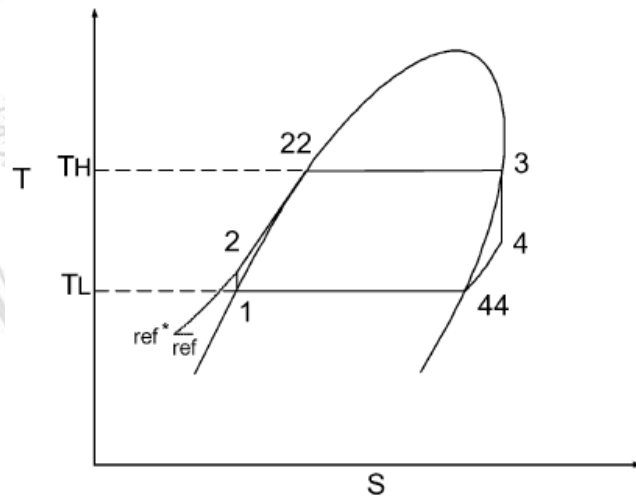


Figure 2.10: Schematic diagram T-s in ORC system (Luis *et al.*, 2004)

In that respect, differentiating Equation 2.21 with respect to T_H yields the following approximately,

$$\frac{ds}{dT_h} \approx \frac{C_P}{T_h} + 2 \frac{d(\Delta H_h)}{d(T_h^2)} - \frac{\Delta H_h}{T_h^2} \quad 2.23$$

By exploitation of the Watson relation between ΔH_h and T_h ,

$$\Delta H_{h,i} = \Delta H_{h,ii} \left(\frac{1 - T_{r,hi}}{1 - T_{r,hii}} \right)^n \quad 2.24$$

where $T_{wf,hi} (= T_{h,i}/T_c)$ and $T_{wf,hii} (= T_{h,ii}/T_c)$ denote the reduced vaporizing temperatures. $\Delta H_{h,i}$ and $\Delta H_{h,ii}$ represent the enthalpies of vaporization at states i and ii, respectively; the exponent n is suggested to be 0.375 or 0.380 by Watson relation. Substituting Equation 2.22 into Equation 2.23 yields,

$$\xi = \frac{C_p}{T_h} - \left(\frac{\frac{n \cdot T_{wf,h}}{1 - T_{wf,h}} + 1}{T_h^2} \right) \Delta H_h \quad 2.25$$

where $\xi = ds / dT_h$ is the slope of saturated vapor curve on T-S diagram. Types of working fluids can be predicted by the above expression. That is, $\xi > 0$: a dry fluid, $\xi \sim 0$: an isentropic fluid, and $\xi < 0$: a wet fluid. Table 2.1 illustrates types of some working fluids from thermodynamic data (Lui et al., 2004) and the results predicted by Equation 2.23. As seen in the table, reasonably good agreement between thermodynamic data and predicted results by Equation 2.24 is shown. From Table 1, we can find that not all the organic working fluids belong to dry or isentropic type. For example, ethanol is a wet fluid. This can be explained from Equation 2.25, where n may become negative as ΔH_h is large enough. This implies the working fluid is in fact a wet type. In addition to the above direct consequence, the actual cause is related to the chemical structure of the working fluids. For working fluids such as water showing strong attraction among molecules, ΔH_H is comparatively large. Hence, molecules having hydrogen bonds interactions like water, ammonia, and ethanol give rise to large ΔH_H and become wet types.

Table 2.1: Physical, safety, and environmental data of the few working fluids (Tchanche *et al.*, 2009)

Substance	Type	Physical properties					Environmental data			Safety data ASHRAE34 safety group
		Molecular mass (kg/kmol)	T_{bp}^a (°C)	T_c^b (°C)	P_{bp}^c (MPa)	Atm life time (y)	ODP ^d	GWP ^e (100y)		
1 RC318	d	200.03	-6.0	115.2	2.778	3200	0	10,250	A1	
2 HFC-600a	d	58.12	-11.7	135.0	3.647	0.019	0	20	A3	
3 CFC-114	d	170.92	3.6	145.7	3.289	300	1	10,240	A1	
4 HCFC-600	d	58.12	-0.5	152.0	3.769	0.018	0	20	A3	
5 HFC-601	d	72.15	36.1	196.5	3.364	0.01	0	20	-	
6 CFC-113	d	187.38	47.6	214.1	3.439	85	1	6,130	A1	
7 Cyclohexane	d	84.16	80.7	280.5	4.075	n.a.	n.a.	n.a.	A3	
8 HFC-290	w	44.10	-42.1	96.7	4.247	0.041	0	20	A3	
9 HFC-407C	w	86.20	-43.6	86.8	4.597	n.a.	0	1,800	A1	
10 HFC-32	w	52.02	-51.7	78.1	5.784	4.9	0	675	A2	
11 CFC-500	w	99.30	-33.6	105.5	4.455	n.a.	0.738	8,100	A1	
12 HFC-152a	w	66.05	-24.0	113.3	4.520	1.4	0	124	A2	
13 R717 (ammonia)	w	17.03	-33.3	132.3	11.333	0.01	0	1	B2	
14 Ethanol	w	46.07	78.4	240.8	6.148	n.a.	n.a.	n.a.	n.a.	
15 Methanol	w	32.04	64.4	240.2	8.104	n.a.	n.a.	n.a.	n.a.	
16 R718 (water)	w	10.20	100.0	374.0	22.064	n.a.	0	1	A1	
17 HFC-134a	i	102.03	-26.1	101.0	4.059	14	0	1,430	A1	
18 CFC-12	i	120.91	-29.8	112.0	4.114	100	1	10,890	A1	
19 HCFC-123	i	152.93	27.8	183.7	3.668	1.3	0.02	77	B1	
20 HCFC-141b	i	116.95	32.0	204.2	4.249	9.3	0.12	725	n.a.	

n.a., non-available.

T_{bp}^a is the normal boiling point, °C

T_c^b is the critical temperature, °C

P_{bp}^c is the critical pressure, MPa

ODP^d is the ozone depletion potential, relative to CFC-11.

GWP^e is the global warming potential, relative to CO₂.